resolution genomic analysis of immortal human cells and tumor cells using array-based comparative genomic hybridization. Environmental Mutagen Society 37th Annual Meeting (2006.9)

Luan Y., Honma M., Suresh T., Kogi M., Yamaguchi T., Suzuki T. CGH and SNP array are powerful tools for chromosome analysis. Environmental Mutagen Society 37th Annual Meeting (2006.9)

Matsufuji H., Chino M., Hayashi M., Honma M., Yamagata K. Genotoxicity of quercetine in the presence of reactive oxygen species using human lymphoblastoid TK6 cells. Environmental Mutagen Society 37th Annual Meeting (2006.9)

本間正充、鈴木雅雄、谷田貝文夫　染色体切断に対する放射線影響の検討　日本宇宙生物科学会第20回大会(2006.9)

梅林志浩、菅澤薫、本間正充、島津徹、鈴木ひろみ、石岡憲昭、岩本正哉、谷田貝文夫　放射セン適応応答による突然変異の抑制 ISS 利用実験計画：宇宙環境の突然変異に及ぼす影響の推定　日本宇宙生物科学会第20回大会(2006.9)

Honma M., Sakuraba M., Koizumi T., Takashima Y., Sakamoto H. and Hayashi M., Requirement of p53 for maintenance of chromosome integrity against DNA double strand breaks. DNA Repair 2006 (2006.9)

本間正充　DNA2本鎖切断修復によるゲノム安定化機構　日本環境変異原学会第35回大会(2006.11)

斉藤美香、高島良生、坂本浩子、林　真、松藤寛、山形一雄、本間正充　簡便な in vitro コメット試験法の確立とその評価　日本環境変異原学会第35回大会(2006.11)

小山直己、加藤竜也、本間正充、林　真、増田修一、木苗直秀　ヒトリンパ芽球トランスジェニック細胞を用いたアクリルアミドおよびグリシダミドの遺伝毒性試験　日本環境変異原学会第35回大会(2006.11)

谷田貝文夫、梅林志浩、鈴木雅雄、岩木正哉　染色体特定部位 DSB の修復：低線量／低線量率ガンマ線照射による影響　日本環境変異原学会第35回大会(2006.11)

高島良生、小泉朋子、櫻庭真弓、林　真、本間正充　ライブセルイメージングによる小核の運命の追跡　日本環境変異原学会第35回大会(2006.11)

松藤寛、千野誠、本間正充、林　真、山形一雄　ヒトリンパ芽球細胞株 TK6 を用いた亜硝酸ナトリウムと抗酸化剤の複合遺伝毒性　日本環境変異原学会第 35 回大会(2006.11)

Honma M. DNA double strand break inducing chromosome instability and its genetic consequences. International Conference on Biomarkers in Health and Environmental Management & XXXII Annual Meeting Environmental Mutagen Society of India (2007.1)

Honma M. DNA double strand breaks inducing chromosome instability in

p53-deficient human cells. Key Stone Symposia -Genome Instability and Repair (2007.1)

本間正充：代謝物の遺伝毒性評価　第 34 回日本トキシコロジー学会学術年会 (2007.6)

Honma M.: DNA double strand breaks inducing genomic instability in human cells. 13th International Congress of Radiation Research (2007.7)

Yatagai F., Suzuki M., Ishioka N., Ohmori H., and Honma M.: Repair of dsb at a specific site of chromosome: influence of low-dose/low-dose-rate gamma-rays. 13th International Congress of Radiation Research (2007.7)

Honma M.: Genotoxic assessment of drug metabolite and ICH guideline. Chinese National Conference on Drug Toxicology 2007 (2007.8)

Honma M.: A multi-endpoints in vitro genotoxicity test system consisting of Comet, micronuclei, and gene mutation assays. 6th World Congress on Alternatives & Animal Use in the Life Sciences (2007.8)

Honma M., Takashima Y., Yasui M., Koyama N., Koizumi T., Sakuraba M., Sakamoto H., Sugimoto K., and Hayashi M.: Tracing Micronuclei by Fluorescent Live Cell Imaging Analysis. 37th European Environmental Mutagen Society (2007.9)

Honma M.: Genomic instability caused through breakage-fusion-bridge (BFB) cycle in human cells. The 8th International Symposium on Chromosomal Aberrations (2007.10)

Suzuki T., Luan Y., Praba D., Kogi M., Honma M., Koizumi T., Tanabe S., Sato Y., Suzuki K., and Yamaguchi T.: CGH and SNP arrays; as new tools for detailed analysis of chromosome. The 8th International Symposium on Chromosomal Aberrations (2007.10)

Honma M.: The new ICH guideline on Genotoxicity. 2007 Korean National Institute of Toxicological Research International Symposium (2007.10)

Honma M.: Validation of a humanized in vitro genotoxicity test system. 2007 Korean NTP Workshop (2007.10)

安井学、小山直己、高島良生、小泉朋子、櫻庭真弓、坂本浩子、杉本憲治、林　真、本間正充：ライブセルイメージングを用いたγ線照射による小核形成と追跡　日本放射線影響学会第 47 回大会 (2007.11)

本間正充、櫻庭真弓、林　真：DNA マイクロアレイによる放射線損傷領域のゲノムマッピング　日本放射線影響学会第 47 回大会 (2007.11)

谷田貝文夫、鈴木雅雄、本間正充：　低線量・低線量率γ線照射によるヒトリンパ芽球細胞での変異誘発　日本放射線影響学会第 47 回大会 (2007.11)

Koyama N., Yasui M., Sakamoto H., Sakuraba M., Masuda S., Kinae N., Matsuda T, Hayasi M., and Honma M: Genotoxicity of acryamide expressed via metabolic activation in CYP over-expressing human cells. 1st Asian Conference on Environmental Mutagens & 36th Annual Meeting of the Japanese Environmental Mutagen Society (2007.11)

Yasui M., Suenaga E., Koyama N., Masutani C., Hanaoka F., Gruz P., Shibutani S., Nohmi T., Hayashi M., and Honma M.: Translesion synthesis past 2'-deoxyinosine, a major nitric oxide-induced DNA adduct, by human DNA polymerase η and κ. 1st Asian Conference on Environmental Mutagens & 36th Annual Meeting of the Japanese Environmental Mutagen Society (2007.11)

Yatagai F., Matsumoto H., Honma M.: A possible involvement of bystander effects in the repression of spontaneous mutation induction. 1st Asian Conference on Environmental Mutagens & 36th Annual Meeting of the Japanese Environmental Mutagen Society (2007.11)

Saito M., Matsufuji H., Chino M., Hyashi M., Honma M., and Yamagata K.: Antioxidant activity and potential genotoxicity of flavonoid by using human lymphoblastoid TK6 cells. 1st Asian Conference on Environmental Mutagens & 36th Annual Meeting of the Japanese Environmental Mutagen Society (2007.11)

Arai S., Saito M., Takashima Y., Honma M., and Kojima H.: A new trial for in vitro Comet assay using 3-dementional human epidermal model. 1st Asian Conference on Environmental Mutagens & 36th Annual Meeting of the Japanese Environmental Mutagen Society (2007.11)

Kimura A., Sakamoto H., Hayashi M., Saigo K., Tokado H., and Honma M.: Establishment of a robust in vitro Comet protocol using human lymphoblastoid TL6 cells. 1st Asian Conference on Environmental Mutagens & 36th Annual Meeting of the Japanese Environmental Mutagen Society (2007.11)

Honma M., Yasui M., Koyama N., Koizumi T., Sakuraba M., Sakamoto H., Takashima Y., Sugimoto K., and Honma M.: Visualization od micronuclei by fluorescent cell imaging analysis. 1st Asian Conference on Environmental Mutagens & 36th Annual Meeting of the Japanese Environmental Mutagen Society (2007.11)

Suzuki T., Koizumi T., Prabha D., Luan Y., Honma M., Hamada S., Nakajima M., Watanabe T., and Furihata C.: Collaborative study on the toxicogenomics in JEMS/MMS II: High-throughput qPCR analysis by TaqMan low density array. 1st Asian Conference on Environmental Mutagens & 36th Annual Meeting of the Japanese Environmental Mutagen Society (2007.11)

Honma M.: Background issues initiating a

revision of the current ICH genotoxicity guidance. 1st Asian Conference on Environmental Mutagens & 36th Annual Meeting of the Japanese Environmental Mutagen Society) (2007.11)

村田香織、森山英樹、高島良生、本間正充、岡茂範、杉本憲治：マルチカラーライブセルイメージングにより明らかとなったAurora-B キナーゼ阻害剤 VX-680 の染色体分配ダイナミズムに及ぼす影響　第 30 回日本分子生物学会年会(2007.12)

本間正充：医薬品に不純物として含まれる遺伝毒性物質の分類と許容量　第 35 回日本トキシコロジー学会学術年会(2008.6)

本間正充：ICH における新しい遺伝毒性試験ガイドライン（S2R1）と試験実施タイミング　第 35 回日本トキシコロジー学会学術年会(2008.6)

Honma, M. Ultimate Threshold and Genetic Consequence of A Single Double Strand Break in Human Cells. International Symposium on Genotoxic and Carcinogenic Thresholds (2008.7)

Honma, M. Genome Mapping of Damaged Chromosome Regions Induced by Ionizing Irradiation Using DNA Microarray Analysis. 38th European Environmental Mutagen Society (2008.9)

鈴木孝昌、小木美恵子、小原有弘、本間正充、田邊思帆里、山口照英：SNP および CGH マイクロアレイを用いた c-myc 遺伝子増幅に関する詳細解析　第 67 回日本癌学会総会(2008.10)

谷田貝文夫、菅澤薫、榎本秀一、本間正充：DSB 修復効率からの適応応答の追求　日本放射線影響学会第 51 回大会(2008.11)

本間正充：DNA 二本鎖切断修復と遺伝的不安定性　日本環境変異原学会第 37 回大会(2008.12)

安井　学、本間正充：ヒトリンパ球細胞のゲノム内に導入させた 8-オキソグアニン 1 分子の突然変異誘発能　日本環境変異原学会第 37 回大会(2008.12)

小山直己、木村葵、安井学、高見成昭、高橋美和、今井俊夫、山本歩、汲田和歌子、増村健一、増田修一、木苗直秀、松田知成、能美健彦、本間正充：ライフステージを考慮したアクリルアミドの多臓器遺伝毒性評価　日本環境変異原学会第 37 回大会(2008.12)

斉藤美香、松藤寛、千野誠、林真、本間正充、山形一雄：過酸化水素によって誘導されたヒトリンパ芽球細胞 TK6 の細胞増殖と遺伝毒性に対する天然抗酸化物質の保護効果　日本環境変異原学会第 37 回大会(2008.12)

木村葵、坂本浩子、西郷和彦、洲加本孝幸、本間正充：*In vitro* コメットアッセイプロトコールの検証　日本環境変異原学会第 37 回大会(2008.12)

Wang, J., Sawyer, J., Honma, M., Chen, T., and Moore, M. The Mouse Lymphoma Assay detects recombination, deletion, and aneuploidy. 日本環境変異原学会第 37 回大会(2008.12)

谷田貝文夫、高橋昭久、本間正充、鈴木ひろみ、大森克徳、関真也、橋爪藤子、島津徹、榎本秀一、大西武雄、石岡憲昭：宇宙実験：放射線影響のLOH検出系による解析　日本環境変異原学会第37回大会(2008.12)

鈴木孝昌、小泉朋子、本間正充、中嶋圓、濱田修一、渡辺貴志、降旗千恵：トキシコゲノミクスに関するJEMS/MMS共同研究II：遺伝子傷害性発癌物質の迅速スクリーニング系としてのTaqMan Low Density Arrayの評価　日本環境変異原学会第37回大会(2008.12)

本間正充、櫻庭真弓、汲田和歌子、林真：DNAマイクロアレイによる放射線損傷領域のゲノムマッピング　日本環境変異原学会第37回大会(2008.12)

中嶋圓、鈴木雅也、田中仁、本間正充、林真：*In vitro* コメットアッセイ国際バリデーションデータ解析に関する一考察　日本環境変異原学会第37回大会(2008.12)

安井学、Suzuki, N.、本間正充、Shibutani, S.：一酸化窒素によって形成するDNA付加体の誤塩基対形成メカニズム　第31回分子生物学会(2008.12)

G. 知的所有権の取得状況

なし

別添4

研究成果の刊行に関する一覧表

書籍

著者氏名	論文タイトル名	書籍全体の編集者名	書　籍　名	出版社名	出版地	出版年	ページ
	該当なし。						

雑誌

発表者氏名	論文タイトル名	発表誌名	巻号	ページ	出版年
Kurebayashi, H., Ohno, Y.	Metabolism of acrylamide to glycidamide and their cytotoxicity in isolated rat hepatocytes: protective effects of GSH precursors.	Arch. Toxicol.	80	820-828	2006
Kurebayashi, H., Ohno, Y.	Metabolism and cytotoxity of acrylamide in isolated rat hepatocytes: protective effects of GSH precursors.	Drug Metabol. Rev.	39 S1	246	2007
Woo, G-H., Shibutani, M., Kuroiwa, K., Lee, K-Y., Takahashi, M., Inoue, K., Fujimoto, H., Hirose, M.	Lack of preventive effects of dietary fibers or chlorophyllin against acrylamide toxicity in rats.	Food Chem. Toxicol.	45	1507-1515	2007
Takahashi, M., Shibutani, M., Inoue, K., Fujimoto, H., Hirose, M., Nishikawa, A.	Pathological assessment of the nervous and male reproductive systems of rat offspring exposed maternally to acrylamide during the gestation and lactation periods - a preliminary study.	J. Toxicol. Sci.	33	11-24	2008
Takahashi, M., Shibutani, M., Nakahigashi, J., Sakaguchi, N., Inoue, K., Morikawa, T., Yoshida, M., Nishikawa, A.	Limited lactational transfer of acrylamide to rat offspring on maternal oral administration during the gestation and lactation periods.	Arch. Toxicol.			(In press)

Cho, Y.M., Imai, T., Hasumura, M., Watanabe, N., Ushijima, T., Hirose, M., Nishikawa, A.	Increased H-*ras* mutation frequency in mammary tumors of rats initiated with *N*-methyl-*N*-nitrosourea and treated with acrylamide.	J. Toxicol. Sci.			(In press)
Koyama, N., Sakamoto, H., Sakuraba, M., Koizumi, T., Takashima, Y., Hayashi, M., Matsufuji, H., Yamagata, K., Masuda, S., Kinae, N., Honma, M.	Genotoxicity of acrylamide and glycidamide in human lymphoblastoid TK6 cells.	Mutat. Res.	603	151-158	2006

Arch Toxicol (2006) 80: 820–828
DOI 10.1007/s00204-006-0109-x

METABOLIC ACTIVATION/INACTIVATION

Hideo Kurebayashi · Yasuo Ohno

Metabolism of acrylamide to glycidamide and their cytotoxicity in isolated rat hepatocytes: protective effects of GSH precursors

Received: 26 December 2005 / Accepted: 12 April 2006 / Published online: 13 May 2006

Abstract Acrylamide (AA) is a widely studied industrial chemical that is neurotoxic, mutagenic to somatic and germ cells, and carcinogenic in rodents. The recent discovery of AA at ppm levels in a wide variety of commonly consumed foods has energized research efforts worldwide to define toxicity and prevention. Metabolism and cytotoxicity of AA and its epoxide glycidamide (GA) were studied in the hepatocytes freshly isolated from male *Sprague–Dawley* rats. The isolated hepatocytes metabolized AA to GA. The formation of GA followed Michaelis-Menten kinetic parameters yielded apparent K_m = 0.477 ± 0.100 and 0.263 ± 0.016 mM, V_{max} = 6.5 ± 2.1 and 26.4 ± 3.0 nmol/h/10^6 cells, and CL_{int} = 14 ± 5 and 100 ± 12 µl/h/10^6 cells for the hepatocytes from untreated and acetone-treated rats, respectively. There were lower K_m and marked increases in V_{max} (fourfold) and in CL_{int} (sevenfold) in acetone-treated rat hepatocytes. The data suggest that CYP2E1 played a major role in metabolizing AA to more toxic GA. Both AA and GA induced a concentration- and time-dependent glutathione (GSH) depletion of the hepatocytes. From decreasing rates of GSH contents in hepatocytes, the parameters of glutathione S-transferase (GST) in hepatocytes to AA and GA were calculated to be K_m = 1.4 and 1.5 mM, V_{max} = 21 and 33 nmol/h/10^6 cells, and CL_{int} = 15 and 23 µl/h/10^6 cells, respectively. GA 1.5-times more readily depleted GSH content than AA. GA decreased the viability of hepatocytes at 3 mM, but AA did not. These data indicate that GA is more toxic than AA as assessed by intracellular GSH depletion and loss of viability of hepatocytes. GSH precursors such as *N*-acetylcysteine and methionine provided significant anti-cytotoxic effects on the decrease of GSH content and cell viability of hepatocytes induced by GA and AA.

Keywords Isolated hepatocytes · Acrylamide · Glycidamide · CYP2E1 · Cytotoxicity · GSH precursor

H. Kurebayashi (✉) · Y. Ohno
Division of Pharmacology, Biological Safety Research Center, National Institute of Health Sciences, Kamiyoga 1-18-1, Setagaya, Tokyo 158-8501, Japan
E-mail: kurebaya@nihs.go.jp
Tel.: +81-3-37009762
Fax: +81-3-37076950

Introduction

Acrylamide (AA) is used for industrial and laboratory purposes. AA a monomer form has been shown to have neurotoxic properties in both animals and humans (IPCS 1985). Some studies indicated that chronic AA treatment produced tumors in rats and mice (Johnson et al. 1986; Dearfield et al. 1988; Friedman et al. 1995). International Agency for Research on Cancer (IARC) labeled AA a probable human carcinogen (IARC 1994). The recent finding of AA formation during food processing has triggered worldwide concern (Tareke et al. 2000; Tareke et al. 2002; Mottram et al. 2002; Stadler et al. 2002). The elucidation of the mechanism of AA toxicity on animals and cultured cells, and the search for an inhibitor or protector against AA toxicity are required.

AA is metabolized in vitro and in vivo in mice, rats and humans to the epoxide glycidamide (GA) (Fig. 1). The conversion of AA to GA is saturable, ranging from 50% at very low doses to 13% at 100 mg/kg bw in treated rats (Calleman 1996). Certain circumstantial observations suggested that the metabolic conversion of AA to GA is mediated by P-450 system. The study on the urinary metabolites of AA dosed to CYP2E1-null mice implied that metabolite GA was formed by CYP2E1 (Sumner et al. 1999). P450 2E1 is induced by alcohol and acetone (Forkert et al. 1994). We have tried to verify if presumed reactive metabolite GA is produced in isolated hepatocytes from untreated and acetone-treated rats. We have obtained the in vitro kinetic parameters of the hepatocytes and compared the in vivo toxicokinetic data (Kirman et al. 2003).

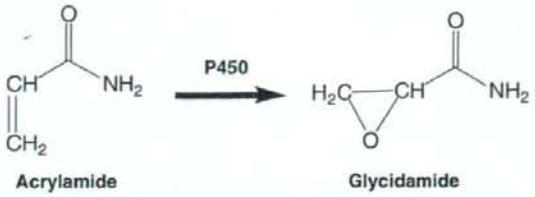

Fig. 1 Metabolism of acrylamide to its epoxide glycidamide

Both AA and GA are detoxified by GSH conjugation, and react directly with hemoglobin in vivo (Calleman et al. 1990), but DNA adducts result only from the formation of GA (Segerbäck et al. 1995). GA is classified as a potential human carcinogen and genotoxicant. Reduced glutathione (GSH) plays an important role in hepatocytes defense (Kedderis 1996; Reed 1994). GSH can act as an alternative nucleophile for nucleophilic portions of proteins and DNA, and thus afford protection against toxic electrophiles within the cell. The most common pathway of GSH depletion in xenobiotic toxicity is excessive consumption of GSH without recovery (Castell et al. 1997). Severe GSH depletion leaves cells more vulnerable to oxidative damage, which causes progressive deterioration of macromolecules, cell structure and may lead to cell death (Reed 1994). GSH level could therefore determine the cytotoxicity of a xenobiotic and its ultimate effects on cell survival.

In this context, we report on the toxicity of AA and GA in freshly isolated rat hepatocytes in relation to cellular GSH status, to investigate possible mechanisms by which AA causes damage in rat hepatocytes. We would like to know whether GA mediates the toxic effects of AA. We have tested the state of cytotoxic marker by cytoplasmic enzyme lactate dehydrogenase (LDH) release and antioxidant estimation of GSH in isolated hepatocytes. Another objective of this study is to investigate the in vitro protective ability of low molecular weight thiols and ascorbic acid (Asc) against the AA- and GA-mediated toxicity on the hepatocytes, because low molecular weight thiols protected against allyl alcohol-induced toxicity on the isolated hepatocytes (Ohno et al. 1985). This study firstly demonstrates the hepatocellular metabolite of AA, i.e., GA and their toxic effects using the same isolated hepatocytes.

Materials and methods

Chemicals

Acrylamide (2-propenamide), for electrophoresis, of 99.9% purity was obtained from Kanto Chemical Co., Inc., (Tokyo, Japan). Glycidamide (GA) of more than 95% purity was obtained from LKT Laboratories, Inc. (West in St. Paul, MN). Reduced glutathione (GSH), *N*-acetyl-L-cysteine (NAC) and L-methionine (Met) were obtained from Sigma Chemical, Co. (St. Louis, MO). Collagenase A was obtained from Boehringer-Mannheim, (Mannheim, Germany). All other chemicals were reagent grade of the highest laboratory purity available.

Animals and treatments

Male Sprague–Dawley rats 6 weeks of age were purchased from SLC Japan Co. (Shizuoka, Japan). Rats were acclimatized for more than 1 week before use, housed under appropriate conditions (23± 2°C, 55 ± 5% humidity) with a 12:12 h light/dark cycle, and provided of pelleted rodent chow and tap water ad libitum. One subset of male rats received 1% acetone in drinking water for 5 days prior to cell preparation to specifically induce CYP2E1 (Forkert et al. 1994).

Isolation, culture of rat hepatocytes

The method described by Seglen (1973) was followed for isolation of hepatocytes, with minor modifications. Freshly isolated hepatocytes were obtained by in situ liver perfusion with collagenase from male Sprague-Dawley rats (8–10 w) weighing 200–250 g. The abdomen of the rat was opened under ether anesthesia and the portal vein cannulated with a plastic catheter (18G × 2") (Terumo Co., Inc., Tokyo, Japan). Liver was perfused with Ca^{2+} and Mg^{2+}-free Krebs Ringer and 25 mM HEPES buffer (KRHB) (pH 7.4) containing 0.5 mM EGTA at 37°C at a flow rate of 40 ml/min for 10 min. Thereafter, a second perfusion with 30 ml/min of Ca^{2+}-free KRHB medium containing collagenase (40 U/ml) at 37°C was performed for 12 min. The excised liver was moved to a Petri dish containing KRHB (pH 7.4), cooled on ice and cells were gently dispersed with forceps. The crude cell suspension was filtered and preincubated for 20 min at 37°C in 50 ml KRHB gassed with carbogen (95% O_2 and 5% CO_2). The hepatocyte suspension was filtered, centrifuged at 50 × *g* for 1 min and washed three times with culture medium KRHB (pH 7.4), which was serum-free. Viable hepatocytes (>85%) were counted with Trypan blue (0.1%, w/v) in KRHB.

Incubation conditions

All incubations with hepatocytes were carried out at a cell density of 1×10^6 cells/ml in 10 ml KRHB (pH 7.4) in 20 ml Ehrenmyer flask at 37°C for 6 h under an atmosphere of air, shaken at 40 oscillations/min. A reaction was started by the addition of AA or GA (final concentration 0, 0.03, 0.1, 0.3, 1, 3 mM) with and without NAC, Met, Asc or GSH. At the designated time points, aliquots (0.030 and 1 ml) of incubation solution were taken for the evaluation of cell viability, metabolites, and GSH content of cells. Aliquots (1 ml) of cell suspensions were collected and immediately centrifuged

at 1,000 × *g* for 10 s. The supernatant solutions were analyzed by HPLC, and the pellet was used for detection of GSH content of cells after washing once with KRHB.

Measurement of glutathione (GSH)

The cellular content of reduced glutathione was determined by a fluorescence assay (Hissin and Hilf 1976) using a fluorescence spectrophotometer Hitachi 650–40 at 350 nm (excitation) and 420 nm (emission). The GSH content was expressed as nmol/10^6 cells or the relative value of the GSH content at starting time as control (= 1).

Measurement of lactate dehydrogenase (LDH) release

Changes in cell viability during incubation were determined by measuring the leakage of LDH from the cell. Cells were incubated with either AA, or its metabolites, GA. The aliquots of cellular suspension (30 µl) were collected to measure LDH activity (LDH_{super}) by the oxidation of NADH. Cells were lysed in 1% Triton X-100. The LDH activity of the total cell lysate was measured (LDH_{super} + LDH_{cell}). The cytotoxicity index was expressed as LDH_{super}/ (LDH_{super} + LDH_{cell}) × 100.

HPLC analysis

HPLC was performed in LC-10A high-performance liquid chromatograph (Shimadzu, Kyoto, Japan) equipped with an SPD-M10AVP photodiode array UV detector. The instrument was fitted with column-1, Shodex MSpak GF-310 4B (50 × 4.6 mm i.d., particle size 6 µm, Shoko Co. Tokyo, Japan); column-2, Hypercarb (100 × 4.6 mm i.d., particle size 5 µm, Thermo Hypersil-Keystone); Column oven temp.: 35°C. Mobile phase composition: water-methanol (95:5). Flow rate; 0.5 ml/min. Switching valve (Nanospace SI-1, Shiseido, Tokyo, Japan) was inserted between column-1 and -2. Sampling time from column-1 to column-2: 1.75–15 min. Elution times of GA and AA were 6.7 and 8.2 min, respectively. The amounts of metabolites formed were determined from these peak areas at a wavelength of 200 nm compared with the standard.

In vitro kinetic studies and statistical analysis

Michaelis-Menten kinetic constants, apparent K_m (mM) and V_{max} (nmol/h/10^6 cells) were determined by regression analysis of Hanes-Wilkinson plots of substrate concentrations between 0.03–3 mM. To ensure a constant reaction rate for GA formation, data of 1 or 2 h incubation were used since the amount of GA almost linearly increased within 2 h. Intrinsic metabolic clearance (CL_{int}) was obtained from ratio of V_{max} /K_m as µl/h/10^6 cells. Toxicokinetic parameters were described as V_{max} (mg/h/kg), K_m (mg/L) and the hepatic clearance, CL_H (ml/h/kg) for 280g rats (Sugita et al. 1981).

Data are expressed as means ± SD ($n \geq 3$) (cells obtained from more than three different rats). The data were analyzed for statistical significance using Student's *t* test. *P* values of less than 0.05 were considered to be significant.

Results

Metabolic formation of GA from AA in freshly isolated hepatocytes

Hepatocytes prepared from untreated male Sprague-Dawley rats were incubated with 0.03–3 mM AA in KRHB (pH 7.4) at 37°C for 6 h under an atmosphere of air. Incubation of AA with the isolated rat hepatocytes yielded a peak with a retention time identical to GA in HPLC analyses. The formation of GA was almost linear within 2 h and gradually decreased after 4-h incubation (Fig. 2a). GA amounted to 10 and 2.5% of the original AA at 0.03 and 1 mM for 6 h, respectively.

There were marked increases in rates of GA formation in hepatocytes isolated from acetone-treated rats (Fig. 2b). The formation rate of GA was 4.1–6.3 (4.9 ± 1.0, N = 20) times greater at the equimolar concentration in the hepatocytes of acetone-treated rats than untreated rats. AA was metabolized by the rat hepatocytes and GA amounted to 25 and 7.5% of AA at 0.03 and 1 mM after 6 h incubation, respectively.

We obtained Michaelis-Menten kinetic parameters, K_m and V_{max} from 1 or 2 h incubation data in each experiment. In the hepatocytes from untreated rats, the formation of GA yielded apparent K_m = 0.477 ± 0.100 mM, V_{max} = 6.5 ± 2.1 nmol/h/10^6 cells, and CL_{int} = 14 ± 5 µl/h/10^6 cells (Table 1).

In the hepatocytes from acetone-treated rats, there were lower K_m = 0.263 ± 0.016 mM and marked increases in V_{max} = 26.4 ± 3.0 nmol/h/10^6 cells and CL_{int} = 100 ± 12 µl/h/10^6 cells (Table 1). The parameters increased markedly at V_{max} (fourfold) and CL_{int} (sevenfold) in the hepatocytes from acetone-treated rats.

Effects of AA on the hepatocytes

The hepatocytes isolated from untreated rats contained 35.2 ± 2.2 nmol GSH/10^6 cells at the beginning (Fig. 3a). Although it slowly decreased in absence of AA, GSH content of hepatocytes rapidly decreased during incubation with AA. AA (3 mM) rapidly decreased 42% of GSH content after 1 h of incubation. Significant decreases ($P < 0.05$) in GSH content occurred in the hepatocytes exposed to AA at 1 and 3 mM after 1–6 h incubation. Difference was not significantly observed under 0.3 mM AA.

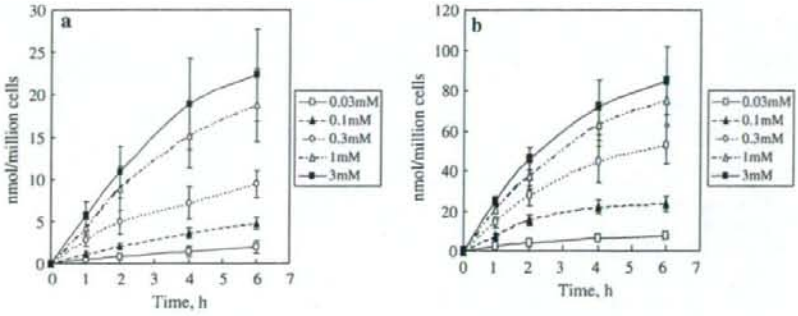

Fig. 2 Formation of glycidamide from acrylamide (AA) in the hepatocytes freshly isolated from untreated rats (**a**) and acetone-treated rats (**b**). The hepatocytes were incubated with different concentrations of AA through 6 h. At the designated time points, samples were taken for determination of metabolites. The values represent mean ± SD of four rats. *Open squares*, 0.03 mM AA; *closed triangles*, 0.1 mM AA; *open circles*, 0.3 mM AA; *open triangles*, 1 mM AA; *closed squares*, 3 mM AA

Table 1 Kinetic parameters of metabolism of acrylamide to glycidamide in the freshly isolated rat hepatocytes

Parameters	Hepatocytes		Acetone-induced/ control
	Control	Acetone-induced	
V_{max} (nmol/h/10^6 cells)	6.5 ± 2.1	26.4 ± 3.0*	4.1
K_m (mM)	0.477 ± 0.100	0.263 ± 0.016*	0.55
V_{max}/K_m (µl/h/10^6 cells)	13.9 ± 4.8	100 ± 12*	7.2

Data are the mean ± SD of four rats
*$P < 0.05$ significantly different from control value

The hepatocytes of acetone-treated rats contained 40.4 ± 3.6 nmol GSH/10^6 cells in the beginning (Fig. 3b). The significant decreases were observed as early as 1 h more than 0.3 mM AA after 2 h. Difference was not significant under 0.1 mM AA in GSH content of the hepatocytes from acetone-treated rats.

The toxicity of AA was evaluated as cell viability by measuring the leakage of LDH enzyme from the hepatocytes after incubation with 6 levels of AA (0, 0.03, 0.1, 0.3, 1, 3 mM) at 37°C. AA did not influence the viability of the hepatocytes prepared from untreated rats and acetone-treated rats, though the cell viability slowly declined during the incubation with and without AA.

Effects of GA on the hepatocytes

The toxicity of GA was evaluated as cell viability of untreated rats after incubation with six levels of GA (0–3 mM) through 6 h (Fig. 4a). We had no effect on cell viability under 1 mM GA, but 3 mM GA significantly decreased the viability of hepatocytes after 4 h (to 12%) and 6 h (to 2%).

The GSH content of the hepatocytes slowly decreased during incubation in absence of GA, but rapidly decreased in presence of GA (Fig. 4b). GA (1 mM and 3 mM) decreased 59 and 86% of GSH content after 1 h.

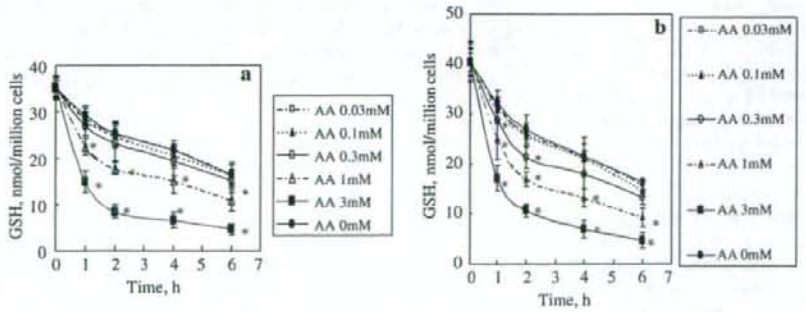

Fig. 3 Effect of acrylamide (AA) on cellular glutathione content of the hepatocytes freshly isolated from untreated rats (**a**) and acetone-treated rats (**b**). The hepatocytes were incubated with different concentrations of AA through 6 h. At the designated time points, samples were taken for determination of glutathione content. Data are the mean ± SD of four rats; *$P < 0.05$ significantly different from control value. *Open squares*, 0.03 mM AA; *closed triangles*, 0.1 mM AA; *open circles*, 0.3 mM AA; *open triangles*, 1 mM AA; *closed squares*, 3 mM AA; *closed circles*, 0 mM AA

GA more rapidly decreased the GSH content of hepatocytes than AA did. More than 0.3 mM GA significantly decreased the GSH content of hepatocytes during 1–6 h incubation. The decrease in GSH content occurred in GA concentration- and time-dependent manner.

Effects of GSH, NAC, Met and Asc on GA toxicity

We have tested whether low molecular weight thiols and Asc have the protective effects on GA-mediated toxicity in isolated hepatocytes. GA (3 mM) significantly decreased the hepatocyte viability (Fig. 4a). The addition of NAC and Met to 3 mM GA medium significantly inhibited the decrease of the cell viability by ca. 40% of the initial value at 4 and 6 h (Fig. 5a). The addition of GSH and Asc to the medium gave some increases ca. 20–30% in the cell viability at 4 h, but did not keep any effect after 6 h.

As significant decreases of cellular GSH contents occurred in the hepatocytes exposed to GA at 1 and 3 mM (Fig. 4b), we have tested whether GSH, NAC, Met and Asc have the role of exogenous antioxidant and protective effects on GA-mediated toxicity on decrease of GSH content of hepatocytes.

The addition of NAC and Met to the medium of 3 mM GA increased the GSH content of hepatocytes from 5% to 40–46% (of the initial value) at 2 h (Fig. 5b). The small increases of 12 and 8% in cellular GSH content were observed at 2 h by addition of GSH and Asc, respectively.

The addition of NAC and Met to 1 mM GA medium efficiently inhibited the decrease of cellular GSH content by ca. 40% during 2–6 h (Fig. 6). The addition of GSH to 1 mM GA gave ca. 20% increase in the GSH content during 2–6 h. The addition of Asc gave a slight increase at 1 and 2 h. Co-incubation of GA with NAC and Met in hepatocytes provided significant anti-cytotoxic effects induced by GA.

Effects of GSH, NAC, Met and Asc on AA toxicity on GSH content of hepatocytes

We have incubated the hepatocytes with and without GSH, NAC, Met and Asc to investigate their in vitro protective ability against the AA-mediated toxicity. AA (3 mM) significantly decreased the GSH content of hepatocytes (Fig. 7). The addition of NAC or Met to the medium of 3 mM AA inhibited the decrease of the GSH content of hepatocytes by ca. 30% (of the initial value) during 2–4 h. The addition of GSH or Asc to 3 mM AA inhibited the decrease of GSH content by 5–7% at 2 h. NAC and Met exerted the protective effect on AA toxicity on GSH content of hepatocytes.

Role of glutathione S-transferase (GST) in the hepatocytes on GSH decreasing reaction

By incubation of GSH and AA (or GA) in buffer (pH = 7.4) without the hepatocytes, the levels of GSH decreased very slowly (< 0.5% of 1 mM GSH/h). The GSH content of the hepatocytes rapidly decreased in the presence of AA (Fig. 3) and GA (Fig. 4b). We thought that GST in the hepatocytes played the role on conjugating AA and GA with GSH and obtained kinetic parameters for GST (Table 2) from the first 1 h decreasing rates of GSH content in the hepatocytes. The calculated values toward AA were the apparent K_m = 1.44 ± 0.20 and 1.15 ± 0.26 mM, V_{max} = 21.2 ± 2.1 and 20.2 ± 3.0 nmol/h/10^6 cells, CL_{int} = 14.7 ± 0.6 and 17.7 ± 1.6 µl/h/10^6 cells in the hepatocytes of untreated and acetone-induced rats, respectively.

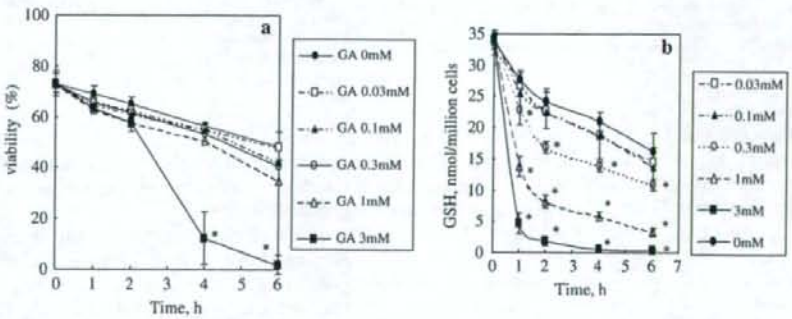

Fig. 4 Effect of glycidamide (GA) on viability (**a**) and glutathione content (**b**) of hepatocytes isolated from untreated rats. The hepatocytes were incubated with different concentrations of GA through 6 h. At the designated time points, samples were taken for determination of LDH leakage and glutathione content. Data are the mean ± SD of four rats; $^*P < 0.05$ significantly different from control value. *Closed circles*, 0 mM GA; *open squares*, 0.03 mM GA; *closed triangles*, 0.1 mM GA; *open circles*, 0.3 mM GA; *open triangles*, 1 mM GA; *closed squares*, 3 mM GA

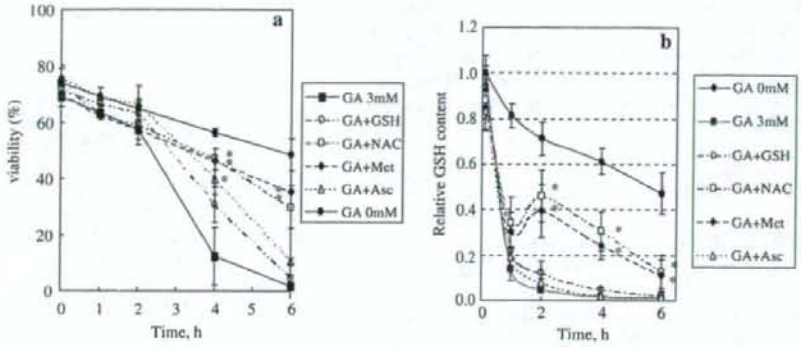

Fig. 5 Effects of *N*-acetylcysteine, methionine, ascorbic acid and GSH on decrease of viability (**a**) and glutathione content (**b**) of the hepatocytes incubated with 3 mM GA. At the designated time points, samples were taken for determination of LDH leakage and glutathione content. Data are the mean ± SD of three rats; $*P < 0.05$ significantly different from 3 mM GA value. *Closed squares*, 3 mM GA; *open circles*, 3 mM GA plus 0.5 mM GSH; *open squares*, 3 mM GA plus 0.5 mM *N*-acetylcysteine; *closed diamonds*, 3 mM GA plus 0.5 mM methionine; *open triangles*, 3 mM GA plus 0.5 mM ascorbic acid; *closed circles*, 0 mM GA

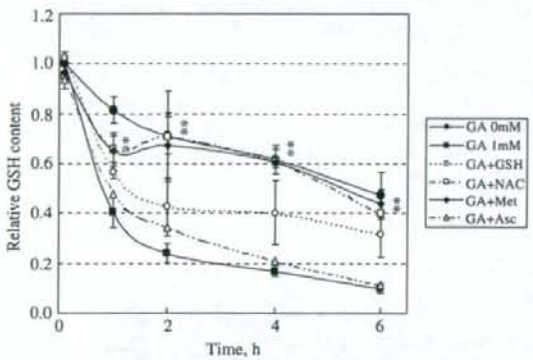

Fig. 6 Effects of *N*-acetylcysteine, methionine, ascorbic acid and GSH on decrease of glutathione content of the hepatocytes incubated with 1 mM glycidamide (GA). Data are the mean ± SD of three rats; $*P < 0.05$ significantly different from 1 mM GA value. *Closed squares*, 1 mM GA; *open circles*, 1 mM GA plus 0.5 mM GSH; *open squares*, 1 mM GA plus 0.5 mM *N*-acetylcysteine; *closed diamonds*, 1 mM GA plus 0.5 mM methionine; *open triangles*, 1 mM GA plus 0.5 mM ascorbic acid; *closed circles*, 0 mM GA

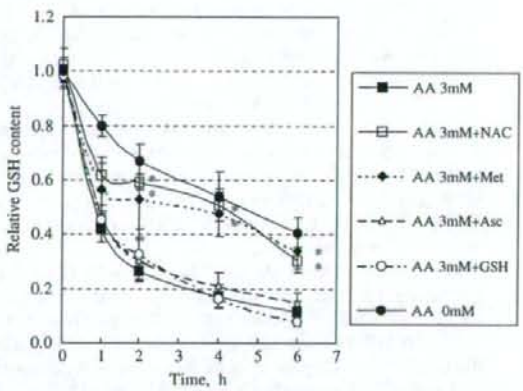

Fig. 7 Effects of *N*-acetylcysteine, methionine, ascorbic acid and GSH on decrease of glutathione content of the hepatocytes incubated with 3 mM acrylamide (AA). Data are the mean ± SD of three rats; $*P < 0.05$ significantly different from 3 mM AA value. *Closed squares*, 3 mM AA; *open squares*, 3 mM AA plus 0.5 mM *N*-acetylcysteine; *closed diamonds*, 3 mM AA plus 0.5 mM methionine; *open triangles*, 3 mM AA plus 0.5 mM ascorbic acid; *open circles*, 3 mM AA plus 0.5 mM GSH; *closed circles*, 0 mM AA

The values toward GA were the apparent K_m = 1.48 ± 0.2 mM, V_{max} = 33.0 ± 3.2 nmol/h/10^6 cells, and CL_{int} = 22.6 ± 4.1 µl/h/10^6 cells in the hepatocytes of untreated rats (Table 2). They were 1.5-times higher at V_{max} and CL_{int} toward GA than AA.

Discussion

The liver is very active in metabolizing foreign compounds. The biotransformation of xenobiotics by the liver involves chemical modifications that totally increase their water solubility thereby facilitating their elimination from the organism in bile and urine. These reactions may result in the formation of compounds of greater toxicity.

Isolated hepatocytes are an extensively used model for the study of liver toxicity. They are very advantageous in some points, but their cytochrome P-450 content declines over the first 72 h in culture (Grant et al. 1985; Turner and Pitot 1989), reducing xenobiotic metabolizing capability and consequently the validity of this model. Then, we limited the exposure time to the tested compounds to 6 h, also considering that the progression of biochemical and structural alterations

Table 2 Kinetic parameters of metabolism of acrylamide and glycidamide with GSH by GST in the freshly isolated rat hepatocytes

Parameters	Acrylamide		Glycidamide
	Hepatocytes		Hepatocytes
	Control	Acetone-induced	Control
V_{max} (nmol/h/10^6 cells)	21.2 ± 2.1	20.2 ± 3.0	33.0 ± 3.2*
K_m (mM)	1.44 ± 0.20	1.15 ± 0.26	1.48 ± 0.21
V_{max}/K_m (μl/h/10^6 cells)	14.7 ± 0.6	17.7 ± 1.6	22.6 ± 4.1*

Data are the mean ± SD of three rats
*$P < 0.05$ significantly different from acrylamide control value

following the exposure to a xenobiotic is much more rapid in vitro than in vivo.

In the present study, we have directly shown that the isolated rat hepatocytes metabolize AA to GA. The formation of GA was almost linear within 2 h (Fig. 2). The kinetic parameters obtained at Table 1 can be described as V_{max} = 2.6 mg/h/kg, K_m = 34 mg/L and CL_H = 75 ml/h/kg for 280 g of rats (Table 3) (Sugita et al. 1981). These values were consistent with Kirman et al. (2003) who estimated metabolism of AA via cytochrome P-450 as V_{max} of 1.6 mg/h/kg and a K_m of 10 mg/L based on the proportion of various metabolites found in rat urine.

We first have shown that the hepatocytes of acetone-treated rats more rapidly metabolize AA to GA than untreated rats (Fig. 2). The parameters increased markedly at V_{max} (fourfold) and CL_{int} (sevenfold) for acetone-treated rats (Table 1). They could be described as V_{max} = 10 mg/h/kg, K_m = 19 mg/L and CL_H = 550 ml/h/kg (Table 3) (Sugita et al. 1981).

This induction rate was consistent with fivefold increase of V_{max} for acrylonitrile epoxidation in liver microsomes from acetone treated rats (Kedderis et al. 1993) and 3.7-fold increase of CYP2E1 activity as hydroxylation of p-nitrophenol in microsomes from murine liver after chronic acetone administration (Forkert et al. 1994). Further, the addition of 0.2% methanol (v/v) to the incubation medium severely inhibited the formation of GA from AA (unpublished data). The solvents such as methanol are known as substrates and inhibitors to CYP2E1. These data indicated the main contribution of CYP2E1 to this metabolic pathway in hepatocytes (Fig. 1).

Table 3 Kinetic parameters of metabolism of acrylamide and glycidamide by P450 and GST in rat (280 g)

Parameters	P450		GST		
	Acrylamide to glycidamide		Acrylamide + GSH		Glycidamide + GSH
	Control rats	Acetone-induced rats	Control rats	Acetone-induced rats	Control rats
V_{max} (mg/h/kg)	2.5	10	8.3	7.9	13
k_m (mg/l)	34	19	103	82	105
CL_H (ml/h/kg)	75	554	81	97	123

The parameters were estimated from Tables 1 and 2
CL_H, hepatic clearance

We have shown that AA exerted the significant decreases in cellular GSH content of hepatocytes exposed to more than 1 mM AA for untreated rats and more than 0.3 mM AA for acetone-treated rats (Fig. 3). Toxic effect of AA on cellular GSH contents seemed more sensitive in hepatocytes of acetone-treated rats where GA was more rapidly produced from AA.

Both AA and GA induced a concentration- and time-dependent GSH depletion in the hepatocytes (Figs. 3, 4b). The GSH depletion was clearly more marked by GA than AA at high concentration studied. Further, GA (3 mM) caused the decrease of the viability of the hepatocytes (Fig. 4a). Then, the data showed that GA was more cytotoxic than AA. This may be owing to the reaction rate of GA with cellular GSH 50% higher than that of AA (Table 2).

GSH can act as an alternative nucleophile for nucleophilic portions of proteins and DNA, and thus afford protection against toxic electrophiles within the cell. The great majority of the reactions of electrophiles with GSH are detoxication processes. Depletion of GSH may render cells more susceptible to oxidative damage. Low molecular weight thiols protected against allyl alcohol-induced toxicity to the isolated hepatocytes (Ohno et al. 1985). Asc provided anti-oxidant cellular protection against the diquat-induced oxidative toxicity (Nakagawa et al. 1991).

NAC and Met provided significant anti-cytotoxic effect against the decrease of cellular GSH content induced at 3 mM AA (Fig. 7), 3 mM GA (Fig. 5b) and 1 mM GA (Fig. 6). Their protective effects had lag time, meaning they played GSH precursors in the hepatocyte (Reed 1994). Their effects on GSH content looked quite similar at 3 mM AA (Fig. 7) and 1 mM GA (Fig. 6). This also showed that GA was more cytotoxic than AA.

NAC and Met provided significant anti-cytotoxic effect on the decrease of viability of the hepatocytes induced by 3 mM GA. But, GSH and Asc did not efficiently function. Then, the chemical conjugation of GSH and AA or GA was not so rapid outside of hepatocytes to decrease toxicity of AA or GA. Asc would prevent one electron oxidation of GSH, but did not the decrease of GSH content. This meant that GSH converted to GS-conjugates in the hepatocyte.

GA induced the marked GSH depletion in the hepatocytes at 3 mM, and the very low levels of GSH were insufficient to prevent the cell death (Fig. 4). GSH depletion seemed a prerequisite for GA-induced damage in rat hepatocytes. The results are in agreement with previous reports, which described that cytotoxicity as measured by lipid peroxidation, cell necrosis, and loss of intracellular enzymes in vivo and in vitro occurs only if the intracellular concentrations of GSH fall below

10–15% of the initial value when GSH is no longer available for protection (Reed 1994).

Although the hepatocytes from acetone-treated rats more rapidly (fourfold) metabolize AA to GA than untreated rats, there was no difference in cell viability of the hepatocytes. The results imply that the expression of CYP2E1 protein per se does not concomitantly implicate enhanced toxicity of AA to cell viability in our condition up to 3 mM AA, suggesting these lower intracellular GSH levels (> 20%) are sufficient to protect the hepatocytes against cell damage (Reed 1994).

Among the endogenous detoxifying systems, GST plays a critical role in protection against electrophiles (Hayes et al. 2005). GST is an enzyme that participates in the detoxification process due to conjugation reactions between GSH and xenobiotics. By incubation with GSH and AA (or GA) in buffer (pH = 7.4), the levels of GSH decreased very slowly (< 0.5% of 1 mM GSH/h) (Dixit et al. 1981), and the addition of GSH to the medium of AA and GA gave small effects on the GSH content of the hepatocytes (Figs. 5b, 6, 7). Thus, the chemical reaction of GSH and AA (or GA) seemed slow. On the other hands, GSH content of hepatocytes rapidly decreased in the presence of AA (Fig. 3) and GA (Fig. 4b). We have thought that GST should have played a role of conjugating AA and GA with GSH in the hepatocytes (Dixit et al. 1981).

From decreasing rates of GSH content in the hepatocytes with AA, we have calculated the GST parameters to AA (Table 2). We have described them as V_{max} = 8.3 and 7.9 mg/h/kg, K_m = 103 and 82 mg/L and CL_H = 81 and 97 ml/h/kg for rats untreated and acetone-induced, respectively (Table 3) (Sugita et al. 1981). We have obtained GST parameters to GA (Table 2), which could be described as V_{max} = 13 mg/h/kg, K_m = 105 mg/L and CL_H = 123 ml/h/kg for 280 g of rats (Table 3). There were 1.5-fold increase in V_{max} and CL_{int} to GA. The rate of GSH depletion by GA-SG adduct formation was approximately 50% higher than AA-SG adduct formation.

As the metabolic rates from AA to GA or AA-SG conjugate were CL_{int} = 13.9 and 14.7 µl/h/10^6 hepatocytes of untreated rats, the former by CYPs is a little lower than the latter by GST. This is consistent with the result of rat urine that 30% of metabolites were derived from GA, and 70% were from conjugation of AA and GSH (Sumner et al. 1992). We can suppose that the metabolic pathway to GA will increase in CYP2E1-induced animals such as acetone-treated rats (Tables 1, 3).

Doerge et al. (2005) compared the toxicokinetics of AA and GA in serum and tissues of male and female B6C3F1 mice following acute dosing by intravenous and gavage at 0.1 mg/kg AA and GA. They reported liver DNA adduct levels from GA were 40% higher than those from an equimolar dose of AA, and suggested that the conversion of AA to GA is more efficient as dosing rate decreases. These findings are critical to the assessment of genotoxicity of AA at low doses in the food supply, which appears to depend on total exposure to GA. However, the simultaneous intake of AA together with GSH precursor amino acids in food will prevent adverse cellular effects of AA and GA.

In conclusion, we have used the isolated hepatocyte for studying metabolism and toxicity of AA at the same time. We have found that AA was metabolized to GA and confirmed the potential of AA to induce cytotoxicity. The metabolite GA was more cytotoxic than AA. GSH precursors such as NAC and Met protected against the cytotoxicity of AA and GA.

References

Calleman CJ (1996) The metabolism and pharmacokinetics of acrylamide: implications for mechanisms of toxicity and human risk estimation. Drug Metab Rev 28:527–590

Calleman CJ, Bergmark E, Costa LG (1990) Acrylamide is metabolized to glycidamide in the rat: evidence from hemoglobin adduct formation. Chem Res Toxicol 3:406–412

Castell JV, Gomez-Lechon MJ, Ponsoda X, Bort R (1997) In vitro investigation of the molecular mechanisms of hepatotoxicity. Arch Toxicol Suppl 19:313–321

Dearfield KL, Abernathy CO, Ottley MS, Brantner JH, Haynes PF (1988) Acrylamide: its metabolism, developmental and reproductive effects, genotoxicity, and carcinogenicity. Mutat Res 195:45–77

Dixit R, Mukhtar H, Seth P, Murti CR (1981) Conjugation of acrylamide with glutathione catalyzed by glutathione-S-transferases of rat liver and brain. Biochem Pharmacol 30:1739–1744

Doerge DR, Young JF, McDaniel LP, Twaddle NC, Mona I (2005) Churchwell Toxicokinetics of acrylamide and glycidamide in B6C3F1 mice. Toxicol Appl Pharmacol 202:258–267

Forkert PG, Redza ZM, Mangos S, Park SS, Tam SP (1994) Induction and regulation of CYP2E1 in murine liver after acute and chronic acetone administration. Drug Metab Dispos 22:248–253

Friedman MA, Dulak LH, Stedham MA (1995) A lifetime oncogenicity study in rats with acrylamide. Fundam Appl Toxicol 27:95–105

Grant MH, Melvin MA, Shaw P, Melvin WT, Burke MD (1985) Studies on the maintenance of cytochromes P-450 and b5, monooxygenases and cytochrome reductases in primary cultures of rat hepatocytes. FEBS Lett 190:99–103

Hayes JD, Flanagan JU, Jowsey IR (2005) Glutathione S-transferases. Annu Rev Pharmacol Toxicol 45:51–88

Hissin PJ, Hilf R (1976) A fluorometric method for determination of oxidized and reduced glutathione in tissues. Anal Biochem 74:214–226

IARC (1994) Acrylamide. Monographs on the evaluation of carcinogen risk to humans. Some industrial chemicals. International Agency for Research on Cancer, Lyon, France, 60:389–433

IPCS (1985) Environmental health criteria 49, Acrylamide. WHO, Geneva

Johnson KA, Gorzinski SJ, Bodner KM, Campbell RA, Wolf CH, Friedman MA, Mast RW (1986) Chronic toxicity and oncogenicity study on acrylamide incorporated in the drinking water of Fischer 344 rats. Toxicol Appl Pharmacol 85:154–168

Kedderis GL (1996) Biochemical basis of hepatocellular injury. Toxicol Pathol 24:77–83

Kedderis GL, Batra R, Koop DR (1993) Epoxidation of acrylonitrile by rat and human cytochromes P450. Chem Res Toxicol 6:866–871

Kirman CR, Gargas ML, Deskin R, Tonner-Navarro L, Andersen ME (2003) A physiologically based pharmacokinetic model for acrylamide and its metabolite, glycidamide, in the rat. J Toxicol Environ Health A 66:253–274

Mottram DS, Wedzicha BL, Dodson AT (2002) Acrylamide is formed in the Maillard reaction. Nature 419:448–449

Nakagawa Y, Cotgreave IA, Moldeus P (1991) Relationships between ascorbic acid and alpha-tocopherol during diquat-induced redox cycling in isolated rat hepatocytes. Biochem Pharmacol 42:883–888

Ohno Y, Ormstad K, Ross D, Orrenius S (1985) Mechanism of allyl alcohol toxicity and protective effects of low-molecular-weight thiols studied with isolated rat hepatocytes. Toxicol Appl Pharmacol 78:169–179

Reed DJ (1994) Mechanisms of chemically induced injury and cellular protection mechanisms, In: Hodgson E, Levi PE (eds) Introduction of Biochemical Toxicology, Second ed. Appleton & Lange, Norwalk, pp 265–295

Segerbäck D, Calleman CJ, Schroeder JL, Costa LG, Faustman EM (1995) Formation of N-7-(2-carbamoyl-2-hydroxyethyl)guanine in DNA of the mouse and the rat following intraperitoneal administration of [14C]acrylamide. Carcinogenesis 16:1161–1165

Seglen PO (1973) Preparation of rat liver cells. II. Effects of ions and chelators on tissue dispersion. Exp Cell Res 76:25–30

Stadler RH, Blank I, Varga N, Robert F, Hau J, Guy PA, Robert MC, Riediker S (2002) Acrylamide from Maillard reaction products. Nature 419:449–450

Sugita O, Sawada Y, Sugiyama Y, Iga T, Hanano M (1981) Prediction of drug-drug interaction from in vitro plasma protein binding and metabolism. A study of tolbutamide-sulfonamide interaction in rats. Biochem Pharmacol 30:3347–3354

Sumner SC, MacNeela JP, Fennell TR (1992) Characterization and quantitation of urinary metabolites of [1,2,3–13C]acrylamide in rats and mice using 13C nuclear magnetic resonance spectroscopy. Chem Res Toxicol 5:81–89

Sumner SC, Fennell TR, Moore TA, Chanas B, Gonzalez FJ, Ghanayem BI (1999) Role of cytochrome P4502E1 in the metabolism of acrylamide and acrylonitrile in mice. Chem Res Toxicol 12:1110–1116

Tareke E, Rydberg P, Karlsson P, Eriksson S, Tornqvist M (2000) Acrylamide: a cooking carcinogen? Chem Res Toxicol 13:517–522

Tareke E, Rydberg P, Karlsson P, Tornqvist M (2002) Analysis of acrylamide, a food carcinogen formed in heated foodstuff. J Agric Food Chem 50:4998–5006

Turner NA, Pitot HC (1989) Dependence of the induction of cytochrome P-450 by phenobarbital in primary cultures of adult rat hepatocytes on the composition of the culture medium. Biochem Pharmacol 38:2247–2251

The Journal of Toxicological Sciences (J. Toxicol. Sci.)
Vol.33, No.1, 11-24, 2008

Original Article

Pathological assessment of the nervous and male reproductive systems of rat offspring exposed maternally to acrylamide during the gestation and lactation periods – a preliminary study

Miwa Takahashi[1], Makoto Shibutani[1,2], Kaoru Inoue[1], Hitoshi Fujimoto[1], Masao Hirose[1,3] and Akiyoshi Nishikawa[1]

[1]Division of Pathology, National Institute of Health Sciences, 1-18-1 Kamiyoga, Setagaya-ku, Tokyo 158-8501, Japan
[2]Laboratory of Veterinary Pathology, Tokyo University of Agriculture and Technology, 3-5-8 Saiwai-cho, Fuchu City, Tokyo 183-8509, Japan
[3]Food Safety Commission, 2-13-10 Prudential Tower 6th Floor, Nagata-cho, Chiyoda-ku, Tokyo 100-8989, Japan

(Received September 10, 2007; Accepted October 16, 2007)

ABSTRACT — To evaluate the developmental effects of exposure to acrylamide (ACR) on the nervous and male reproductive systems, pregnant Sprague-Dawley rats were given ACR at 0, 50, 100 or 200 ppm in the drinking water from gestational day 10 to postnatal day 21 and histopathological assessment of offspring was performed at weaning and postnatal week 11. Neurotoxicity was quantitatively assessed with reference to nerve fiber density, percentages of degenerated and small caliber axons in the sciatic nerves, and numbers of aberrant dot-like structures immunoreactive for synaptophysin in the cerebellar molecular layer. Although maternal neurotoxicity was evident from 100 ppm, no changes suggestive of neurotoxicity or testicular toxicity were observed in offspring. However, lowering of body weights was dose-dependently observed from birth at the dose levels of ≥50 ppm in males and ≥100 ppm in females. Maternal malnutrition was apparent at ≥100 ppm during the lactation period. Therefore, poor lactational ACR-exposure due to maternal toxicity might account for the lack of ACR-induced offspring toxicity other than retarded body growth.

Key words: Acrylamide; Neurotoxicity; Testicular toxicity; Developmental exposure; Rat

INTRODUCTION

Acrylamide (ACR), a water-soluble vinyl monomer, is widely used to synthesize polymers for industrial applications such as soil conditioning, wastewater treatment, and cosmetic, paper and textile industries (Friedman, 2003). Exposure to monometric ACR results in peripheral neuropathy characterized by ataxia, skeletal muscle weakness, and weight loss, and multifocal neurofilamentous swelling and eventual degeneration beginning from the distal ends of peripheral nerve axons (Spencer and Schaumburg, 1974; Le Quesne, 1985; LoPachin and Lehning, 1994). The initial target appears to be nerve terminals, in both the central and peripheral nervous systems, and the result is autonomic, behavioral, sensory, and motor disturbance (LoPachin *et al.*, 2003), although the underlying mechanisms remain controversial. Additionally, ACR has carcinogenic potential (Dearfield *et al.*, 1988; IARC, 1994), and exerts adverse effects on male reproduction, including dominant lethality, degeneration of testicular epithelial tissue, and impaired fertilization (Sakamoto *et al.*, 1988; Adler *et al.*, 2000; Tyl and Friedman, 2003). It has been demonstrated that reproductive toxicity is not only induced by ACR, but also by glycidamide (GA), an oxidized metabolite of ACR generated by CYP2E1, which exerts clastogenic effects on spermatids (Adler *et al.*, 2000; Costa

Correspondence: Makoto Shibutani (E-mail: shibutan@nihs.go.jp)

et al., 1992; Ghanayem *et al.*, 2005).

Recently, exposure to ACR in foodstuffs has become a worldwide concern because of its generation in a variety of fried and oven-baked foods during cooking through Maillard reactions of sugars with asparagine residues (Mottram *et al.*, 2002; Friedman, 2003). The 64th Joint FAO/WHO Expert Committee on Food Additives concluded that an intake of 1 μg/kg body weight/day of ACR could be taken to represent the average for the general population (WHO/IPCS, 2006). However, infants and small children may be more highly exposed to ACR due to their lower bodyweights and high consumption of snacks, so that their relative ACR intake is estimated to be 2 to 3-fold higher than in adults (WHO/IPCS, 2006). Because toxicity studies of ACR have hitherto mainly been performed using adult animals to mimic occupational exposure, the data for effects during fetal, infantile and pubertal periods are rather limited. Therefore, it is important for risk assessment of ACR exposure in human to evaluate toxicity taking into account physiological differences between adults and fetuses/infants that might influence sensitivity.

Regarding age-related susceptibility to ACR-induced toxicity, data from animal studies are insufficient and the findings are inconsistent (Kaplan and Murphy, 1972; Ko *et al.*, 1999). Placental transfer of ACR has been reported in experimental animals and humans, and the fetal internal level of ACR on a weight-adjusted basis was estimated to be at least equal to that of human mothers (Ikeda *et al.*, 1983; Schettgen *et al.*, 2004). The potential for exposure to ACR through human milk has been demonstrated in a study conducted with two women (Sörgel *et al.*, 2002). It is evident that ACR is a developmental toxicant in rodents, because suppression of offspring body weight results from maternal exposure (Zenick *et al.*, 1986; Field *et al.*, 1990; Wise *et al.*, 1995; Garey *et al.*, 2005). Furthermore, it has been reported that ACR can produce developmental neurotoxicity, such as decreased motor activity and auditory startle responses in Sprague-Dawley (SD) rat offspring, at a maternal gavage dose of 15 mg/kg body weight/day, a daily dose level that can cause neurotoxicity to maternal animals (Wise *et al.*, 1995).

Many previous studies on ACR-induced toxicity during the developmental stages were conducted with the focus on behavioral endpoints, but detailed assessment of changes in target organs/tissues has been scarce. In the present study, we thereby performed a histopathological assessment of the nervous and male reproductive systems of rat offspring exposed maternally to ACR during the gestation and lactation periods. In humans, since exposure to ACR occurs through ingestion of food in general population, it is reasonable to examine toxic effects of such chemicals by oral administration through food or drinking water to experimental animals. In the present study, ACR was administered to maternal rats through drinking water with the dose levels in inducing histologically apparent neurotoxicity and testicular toxicity after 4 weeks administration in adult male SD rats in our previous studies (Lee *et al.*, 2005; Woo *et al.*, 2007).

MATERIALS AND METHODS

Chemicals and animals

ACR was purchased from Sigma (St. Louis, MO, USA; CAS #79-06-1) as a white powder with a purity of >98%. Pregnant CD® (SD) IGS rats were obtained from Charles River Japan Inc. (Kanagawa, Japan) at gestational day (GD) 3 (the day when a vaginal plug was observed was designated as GD 0) and housed individually in polycarbonate cages with wood chip bedding, maintained in an air-conditioned animal room (temperature: 24 ± 1°C, relative humidity: 55 ± 5%) with a 12-hr light/dark cycle. They received powdered basal diet (CRF-1; Oriental Yeast Co., Ltd., Tokyo, Japan) and tap water *ad libitum* during the 1 week acclimatization period.

Experimental design

On GD 10, dams were randomly divided into 4 groups of 3 dams and given ACR at 0, 50, 100 or 200 ppm in the drinking water from GD 10 to postnatal day (PND) 21. The highest dose was chosen since it is known to induce neurotoxicity within 4 weeks in adult male rats of the same strain used in the present study (Lee *et al.*, 2005). Litters were culled randomly to preserve 8 pups, mostly 4 per sex per litter on PND 3. On PND 21, the offspring were weaned, and all dams and half of the pups were killed by exsanguination from the abdominal aorta under deep anesthesia with ether. The remaining offspring were housed up to 4 littermates of each sex per cage, and maintained until postnatal week (PNW) 11.

Daily observation for clinical signs and mortality was conducted throughout the experimental period. In addition, to assess ACR-induced neurological deficits, animals were scored with respect to the appearance of gait abnormalities (Moser, 1991; Shell *et al.*, 1992; Lee *et al.*, 2005) by placing individual animals free in Plexiglas boxes (90 × 90 × 20 cm) for 3 min. Degrees of abnormality were classified into four categories: grade 1 as normal gait; grade 2 as slightly abnormal gait with slight degrees of ataxia, hopping gait, and foot splay; grade 3 as moderately abnormal gait with moderate degrees of ataxia, foot splay and limb abduction; grade 4 as severely affected gait, including inability to support the body weight as well as foot splay.

Body weights of dams and pups were measured twice a week before weaning, and then recorded every week. Maternal food and water consumption was also recorded twice a week during ACR exposure.

The animal protocol was reviewed and approved by the Animal Care and Use Committee of the National Institute of Health Sciences, Japan.

Histopathological assessment

At necropsy, the brain, liver, spleen, kidneys, testes and epididymides were removed and weighed. The trigeminal nerve, spinal cord and skeletal muscle were also removed. In dams, numbers of implantations were also recorded. The brains were fixed in methacarn solution at 4°C overnight, and the testes in Bouin's solution at room temperature overnight. The other organs were fixed in 10% buffered formalin. All were then routinely processed for paraffin embedding, sectioning at 3 μm, and staining with hematoxylin and eosin (HE). For histopathological assessment of axons in the peripheral nerves, the sciatic nerves were exposed and subjected to in situ fixation by immersion in ice-cold 2.5% glutaraldehyde in 0.1 M phosphate buffer (pH 7.4) for 3 min. The portion located at the ankle position was carefully excised and further fixed with fresh fixative overnight, postfixed in 1% osmium tetroxide in the same buffer for 2 hr at 4°C, and embedded in epoxy resin (TAAB Laboratories Equipment Ltd., Berkshire, UK). Semithin sections, 1 μm in thickness, were stained with toluidine blue for light microscopic assessment.

Immunohistochemistry for synaptophisin (SYP) in the cerebellum and skeletal muscle

To evaluate aberrant SYP-immunoreactivity in the cerebellar molecular layer, sections obtained from methacarn-fixed brain slices including the cerebellum were subjected to immunohistochemistry for SYP. Rabbit polyclonal antibody Ab-4 (1: 200, Lab Vision Corp., Fremont, CA, USA) was used as the primary antibody and immunodetection was conducted with the horseradish peroxidase-avidin-biotin complex method utilizing a VECTASTAIN® Elite ABC kit (Vector Laboratories Inc., Burlingame, CA, USA) with 3,3'-diaminobenzidine/H_2O_2 as the chromogen, as described previously (Woo *et al.*, 2007). In addition, SYP-immunoreactivity was also examined in skeletal muscle using formalin-fixed sections to evaluate the distribution of neuromuscular junctions. For antigen retrieval, the sections of skeletal muscle were heated by autoclaving in 10 mM citrate buffer for 5 min before incubation with the primary antibody.

Morphometric assessment

To quantify axonal degeneration and atrophy in the sciatic nerves and SYP-immunoreactive aberrant dot-like structures in the cerebellar molecular layer, digital photomicrographs were taken with a Vanox-S microscope (Olympus Corp., Tokyo, Japan) equipped Fujix Digital Camera System (Fujifilm Corp., Tokyo, Japan). Measurement was then performed using a MacSCOPE image analysis software package (Version 3.61, Mitani Corp. Tokyo, Japan). The total number of axons/unit area and the number of degenerated axons were counted in one cross sectional area at 400 × magnification of toluidine blue-stained specimens from each animal, and the density and the percentage of degenerated axons were calculated. For the evaluation of sciatic nerve atrophy, numbers of myelinated axons sized >3 μm and <3 μm in diameter were also differentially counted, based on an earlier study that showed a shift in the distribution of axon diameters with a peak frequency around 3 μm on ACR treatment (Saita *et al.*, 1996). For evaluation of SYP-immunoreactive aberrant dot-like structures, numbers of dots in the left cerebellar hemisphere were counted following measurement of the length of the cortex in one cross sectional area at 20× magnification and the number of SYP-immunoreactive dots/unit length of the cortex was calculated.

Statistical analysis

In dams, data were collected for up to 3 animals per group. Therefore, maternal body and organ weights, food consumption, reproductive parameters and values for morphometric assessment in the sciatic nerves and cerebellar molecular layer were analyzed by the Student's *t*-test when the variance was proven to be homogenous among the groups using a test for equal variance. If a significant difference in variance was observed, Welch's *t*-test was performed. In pups, variance in data for body and organ weights, and values from morphometric assessment in the sciatic nerves and cerebellar molecular layer were checked for homogeneity by Bartlett's procedure. If the variance was homogeneous, the data were assessed by one-way analysis of variance. If not, the Kruskal-Wallis test was applied. When statistically significant differences were indicated, the Dunnett's multiple test was employed for comparisons between the 0 ppm and ACR-treated groups. With histopathological changes, incidences were compared using the Fisher's exact probability test and severity data were analyzed with the Mann-Whitney's *U*-test.

RESULTS

Maternal toxicity

One dam at 200 ppm was euthanized on PND 2 because of non-delivery and worsening general condition, and therefore, statistical analysis could not be applied in this group because of the small number (n=2). Maternal water consumption was decreased at 200 ppm throughout the gestation and lactation periods, and suppressed water consumption at 100 ppm became evident after delivery (Fig. 1A). Also, food consumption was reduced in a dose-related manner during the lactation period (Fig. 1B). Body weight gain of dams was suppressed at 100 and 200 ppm from the gestation period, and the suppression became more prominent in the later stages of the dosing period (Fig. 2A). Mean daily intake of ACR by dams during the gestation and lactation periods was 9.9 ± 0.5, 16.7 ± 2.1 and 22.2 mg/kg body weight/day at 50, 100, and 200 ppm, respectively. At 200 ppm, a slightly abnormal gait appeared from GD 20 (Fig. 2B). Symptoms advanced with time, and the gait abnormality score of dams receiving 200 ppm reached grade 4 at PND 14. Dams in the 100 ppm group exhibited gait abnormality from PND 14 and progressed to score 3 or 4 at the end of the experiment. No animals in the 0 and 50 ppm groups exhibited any gait abnormality. ACR did not affect the gestation period, number of implantations, live birth ratio and male pup ratio. However, pup body weights at PND 2 were significantly decreased from 50 ppm in males and from 100 ppm in females (Table 1). At the necropsy at PND 21, body weights in the 100 and 200 ppm groups were decreased by 12% (284.3 ± 26.4 g) and 27% (235.5 g), respectively, as compared with the 0 ppm group value (323.6 ± 14.8 g).

Histopathologically, central chromatolysis of ganglion cells in the trigeminal nerves was observed in maternal rats from 50 ppm (Table 2, Fig. 3A and B). Morphometric assessment of the sciatic nerves showed dose-related increases of degenerated axons and myelinated nerves of < 3 μm in diameter from 100 ppm (Table 2, Fig. 3C and D). In the cerebellar molecular layer, increase of dot-like SYP-immunoreactive structures was observed from 100 ppm as reported previously (Fig. 3E and F; Lee *et al.*, 2005; Woo *et al.*, 2007). However, the distribution of SYP-positive neuromuscular junctions in skeletal muscle did not differ among the groups. No treatment-related histopathologic changes were observed in the liver, spleen, kidneys and spinal cord.

Offspring toxicity until weaning

In both male and female pups, no apparent abnormalities were found on clinical observation for neurological deficit before weaning. Significant depression of body weight was however observed from PND 2 through weaning from 50 or 100 ppm in males and from 100 ppm in females (Fig. 4A and B). At necropsy at weaning, body weights of pups in both sexes were significantly decreased from 100 ppm as compared with those of the 0 ppm group, and pups in the 100 and 200 ppm groups showed little milk content in their stomach.

On histopathological analysis of pups at weaning, increase of remaining external granular cells in the cerebellum was found in ACR-exposed groups with statistical significance for the severity at 200 ppm in both sexes (Table 3). The degree of extramedullary hematopoiesis in the liver and spleen was decreased in a dose-dependent manner, with statistical significance from 100 ppm in males and 200 ppm in females. Though not significant, loss of glycogen in cytoplasm of hepatocytes was observed in the liver at 200 ppm in both sexes. In the testes of the 0 ppm-controls, the seminiferous tubules retained 3 to 4 layers of spermatocytes, although spermatogenesis had not started yet at weaning. In contrast, germinal epithelium of the testes in ACR-exposed groups at 100 and 200 ppm featured 1 to 2 layers of spermatocytes or Sertoli cells only, suggesting retardation of spermatogenesis (Fig. 5A and B). There were no treatment-related histopathological changes in the trigeminal nerves, kidneys and epididymides.

Morphometrically, axonal caliber of pups at weaning was totally smaller than that of dams, and a tendency for decrease of the axonal size was found in association with ACR treatment. In the sciatic nerves, increases of axonal density and the percentage of myelinated nerves of < 3 μm in diameter were observed (Table 4). However, percentages of degenerated axons did not differ between the controls and any of the ACR-exposed groups (Fig. 5C and D). There were also no differences in the numbers of dot-like SYP-immunoreactive structures in the cerebellar molecular layer, and the distribution of SYP-positive neuromuscular junctions was unchanged.

Offspring toxicity after weaning

No animal exhibited any gait abnormality on clinical observation after weaning. One female offspring in the 200-ppm group died at PNW 4, but the cause of death was unclear. After weaning, pups in every group showed a constant increase in body weight gain. In male pups, body weights were significantly lowered as compared to the control from 100 ppm in a dose-dependent manner (Fig. 6A). At 50 ppm, statistically significant suppression was also detected on PNW 4 in males. Similarly, statistically significant lowering of body weights was observed in